molecular pharmaceutics

ARTICLE

pubs.acs.org/molecularpharmaceutics

Noninvasive Transdermal Iontophoretic Delivery of Biologically Active Human Basic Fibroblast Growth Factor

S. Dubey, R. Perozzo, L. Scapozza, and Y. N. Kalia*

School of Pharmaceutical Sciences, University of Geneva & University of Lausanne, 30 Quai Ernest Ansermet, 1211 Geneva, Switzerland

Supporting Information

ABSTRACT: Human basic fibroblast growth factor (hbFGF; 17.4 kDa) has shown promise in the treatment of several dermatological conditions; symptomatic improvement was also observed in patients with peripheral arterial disease after arterial infusion. The objective of this study was to demonstrate the feasibility of using transdermal iontophoresis to deliver biologically active hbFGF noninvasively into and across the skin. The protein was cloned, expressed and purified in-house. Porcine skin was used to investigate transdermal iontophoretic transport of hbFGF as a function of current density (0.15, 0.3, and 0.5 mA/cm^2); results were subsequently confirmed using human skin. Cumulative hbFGF permeation and skin deposition were quantified by ELISA. The absence of proteolytic degradation during skin transit was confirmed by SDS−PAGE. Biological activity postdelivery was determined using cell proliferation assays in human foreskin fibroblast (HFF) and NIH 3T3 cell lines. Confocal laser scanning microscopy (CLSM) was used to visualize the distribution of rhodamine-tagged hbFGF in the skin. Cumulative iontophoretic permeation at 0.3 mA/cm^2 was statistically superior to that at 0.15 mA/cm^2; however, there was no further improvement at 0.5 mA/cm^2. Significant skin deposition of hbFGF was observed, and this dominated transport; for example, after iontophoresis for 8 h at 0.5 mA/cm^2, skin deposition (77.74 ± 37.36 μg/cm^2) was 4.4-fold higher than cumulative permeation (17.64 ± 5.18 μg/cm^2). The superior skin deposition may be advantageous for dermatological applications. The HFF and NIH 3T3 cell proliferation assays confirmed that biological activity of hbFGF was retained postdelivery. Coiontophoresis of acetaminophen showed that the dominant transport mechanism switched from electroosmosis to electromigration upon increasing current density from 0.15 to 0.3 mA/cm^2. Experiments using human skin confirmed that iontophoretic permeation of hbFGF across porcine and human membranes was statistically equivalent. CLSM images of rhodamine-tagged hbFGF postiontophoresis indicated that the protein was evenly distributed throughout the epidermis and dermis. In conclusion, the results confirmed that transdermal iontophoresis was indeed able to deliver structurally intact, functional hbFGF noninvasively into and across the skin. The amounts of protein delivered were similar to those in reports from preclinical and clinical studies.

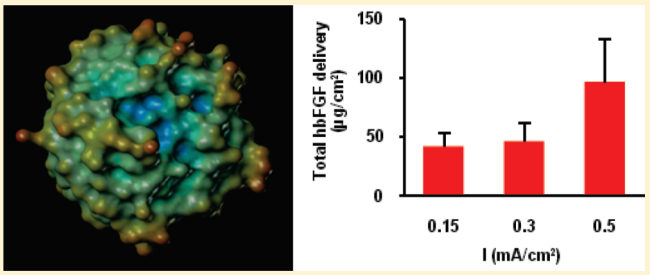

KEYWORDS: transdermal iontophoresis, human basic fibroblast growth factor (hbFGF), protein delivery, noninvasive, formulation, wound healing, peripheral arterial disease

INTRODUCTION

Iontophoresis is an established method for the transdermal delivery of charged low molecular weight therapeutics and peptides.[1,2] Our laboratory has been investigating whether it can also be used for the noninvasive delivery of proteins across the skin, and an earlier report confirmed that it was indeed possible to deliver cytochrome *c* across intact skin using transdermal iontophoresis.[3] More recently, successful delivery of enzymatically active ribonuclease A across porcine and human skin demonstrated that, in addition to structural integrity, biological activity was also retained postiontophoresis.[4] Thus, the challenge now is to determine the physicochemical and structural properties that favor protein electrotransport and to identify potential therapeutic candidates.

Human basic fibroblast growth factor (hbFGF; 155 amino acids) belongs to a large family of structurally related proteins that affect growth, differentiation, migration and survival of a wide variety of cell types. Structural properties including its compact, globular structure and high surface charge distribution suggested that hbFGF might be a good candidate for iontophoretic delivery. Protein globularity is clearly depicted in Figure 1.[5] The protein has an isoelectric point (p*I*) of 9.58, and it carries a net charge of +10 at pH 7.4 (http://www.expasy.ch/tools/protparam.html) by virtue of its 25 positively charged (Arg and Lys) and 15 negatively charged (Asp and Glu) amino acids.

In clinical studies, hbFGF has shown promise in the treatment of various dermatological conditions including skin ulcers,[6−9] burns in both adult and pediatric patients,[10−12] and incisional wounds.[13,14] It has also been tested in phase I clinical trials for the treatment of peripheral arterial disease; although the patients

Received: March 14, 2011
Accepted: June 22, 2011
Revised: May 27, 2011
Published: June 22, 2011

ACS Publications © 2011 American Chemical Society

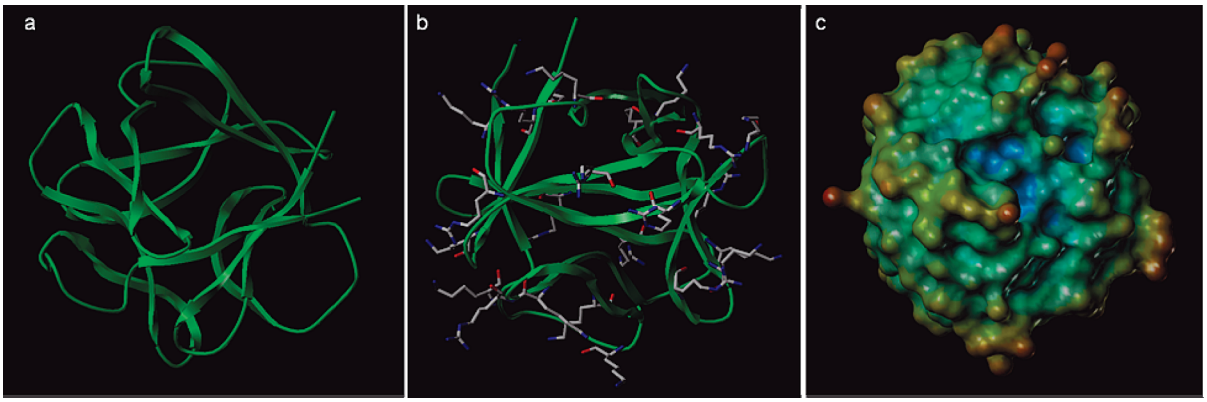

Figure 1. Three-dimensional structure of hbFGF (pdb file: 2FGF).[5] (a) Protein fold: the globularity is clearly discernible. (b) Tertiary structure showing the distribution of positively charged amino acid residues (Arg and Lys). The charged amino acids are predominantly located on the protein surface. (c) Solvent accessible (Connolly) surface showing the electrostatic potential distribution across the molecular surface (red and blue colors represent regions of high positive and negative charge density, respectively). (Structures drawn using SYBYL 8.0.)

showed improvement of symptoms, hbFGF had to be administered by arterial infusion.[15,16] Its short elimination half-life of 46 ± 21 min limits the administration options.[15] Since hbFGF has been reported to induce nephropathy with proteinuria[17] and endothelial growth factors can mediate intraocular neovascularization,[18,19] targeted local therapy may be preferable to systemic parenteral administration.

The specific aims of this study were (i) to clone, express and purify hbFGF, (ii) to develop a stable hbFGF formulation, (iii) to demonstrate that transdermal iontophoresis could be used to deliver intact, biologically active hbFGF across skin, (iv) to investigate the effect of current density on electrotransport, (v) to identify whether electromigration or electroosmosis was the dominant transport mechanism and (vi) to study the distribution of hbFGF in the skin.

EXPERIMENTAL SECTION

Chemicals and Reagents. Acetaminophen (ACM), sodium citrate, rhodamine isothiocyanate, silver wire, silver chloride, RPMi 1640 media and hbFGF (F9786) were purchased from Sigma-Aldrich (Buchs, Switzerland). Sodium chloride, sodium bicarbonate and sodium carbonate were purchased from Fluka (Buchs, Switzerland). Citric acid and 4-(2-hydroxyethyl)-1-piperazineethanesulfonic acid (HEPES) were purchased from Acros Organics (Chemie Brunschwig; Basel, Switzerland). pET100/D-TOPO cloning kit, dNTP mix, and chemocompetent BL21-(DE3)-Star cells were obtained from Invitrogen (Carlsbad, CA). Dulbecco's modified Eagle medium (D-MEM), D-MEM GlutaMAX, fetal bovine serum (FBS) and PenStrep were purchased from Gibco, Invitrogen (Carlsbad, CA). Primers were synthesized by Microsynth (Balgach, Switzerland). Imidazole and XTT sodium salt were purchased from Applichem (Darmstadt, Germany). Yeast extract and tryptone were purchased from Becton Dickinson and Company (Le Pont de Claix, France). The ELISA kit (product number CKH123) used for the quantification of hbFGF was purchased from Cell Sciences (Canton, MA). PVC tubing (3 mm i.d., 5 mm o.d., 1 mm wall thickness) used to prepare salt bridge assemblies was obtained from Fisher Bioblock Scientific S.A. (Illkirch, France). All solutions were prepared using deionized reverse osmosis filtered water (resistivity ≥18 MΩ·cm). All other chemicals were at least of analytical grade.

Skin Source. Porcine ears were obtained from a local abattoir (CARRE; Rolle, Switzerland); the skin was excised (thickness 250 μm; thus, including the epidermis and the upper layers of the dermis) with an air-dermatome (Zimmer; Etupes, France), wrapped in Parafilm and stored at −20 °C for a maximum period of 2 months. Human skin was collected immediately after abdominoplasty (Geneva University Hospital, Geneva), fatty tissue was removed and the skin was wrapped in Parafilm before storage at −20 °C for a maximum period of 3 days. Histological and biophysical studies have demonstrated that porcine skin is an excellent model for human skin;[20−23] investigations into the effect of freezing on human skin have shown that it does not have an impact on integrity.[24,25] The study was approved by the Central Committee for Ethics in Research (CER: 08-150 (NAC08-051); Geneva University Hospital).

Protein Source. hbFGF used in this study was cloned, expressed, purified and characterized in-house. Full details are provided in the Supporting Information.

Protein Formulation. The protein was directly eluted from the pre-equilibrated size exclusion columns in the desired buffer to prepare the different hbFGF formulations (described in Table 1). The final concentration of hbFGF was set at 0.5 mg/mL for each formulation (FS 1−6), and the protein was diluted with the respective elution buffer to achieve this concentration. The first experiments were run to determine the stability of hbFGF in solution after 8 h. Kinetic studies were performed with selected formulations to determine the hbFGF concentration in solution at 0, 2, 4, 6, and 8 h. Stability experiments were performed at room temperature. The hbFGF concentration was quantified by ELISA after incubation of the formulations for 2, 4, 6, and 8 h. The initial concentration of hbFGF (0.5 mg/mL) was taken as 100%, and the concentration measured at each time point was expressed as a percentage of the initial value.

Iontophoretic Setup and Protocol. Customized two-compartment vertical diffusion cells with an additional sampling arm in the receptor compartment were used for the transport studies. Dermatomed skin (area 2.0 cm^2) was clamped between the donor and receptor compartments. The anode, containing 25 mM HEPES, 133 mM NaCl, pH 7.4 (henceforth referred to as HS buffer), was connected to the donor compartment via a salt bridge assembly (3% agarose in 0.1 M NaCl).[26] After a 40 min equilibration period with HS buffer, 1 mL of protein

Table 1. Formulation Compositions Used for hbFGF Solution Stability Studies

formulation	[hbFGF] (mg/mL)	composition	pH	ionic strength (mM)
FS 1	0.5	water	7.0	0
FS 2	0.5	HEPES 25 mM	5.2	9
FS 3	0.5	HEPES 25 mM, NaCl 25 mM	7.4	34
FS 4	0.5	HEPES 25 mM, NaCl 133 mM	7.4	143
FS 5	0.5	HEPES 25 mM, NaCl 133 mM, 0.01% BSA	7.4	143
FS 6	0.5	HEPES 25 mM, NaH_2PO_4 22.2 mM	7.4	64

solution (0.5 mg/mL hbFGF in HS buffer containing 15 mM ACM) was placed in the donor compartment. Acetaminophen (ACM) reported on the electroosmotic solvent flow and enabled the calculation of the contributions of electromigration and electroosmosis to hbFGF electrotransport. The receptor compartment was filled with 12 mL of HS buffer. Constant current was applied using Ag/AgCl electrodes connected to a power supply (Kepco APH 1000M; Flushing, NY). The receptor compartment was stirred at room temperature throughout the experiment; 0.6 mL of the receptor phase was withdrawn every two hours up to 6 h and then hourly until 8 h; each aliquot was replaced with fresh HS buffer. Upon completion of the permeation experiment the diffusion cells were dismantled, and the residual donor solution was removed from the skin surface by washing in running water; hbFGF retained in the skin was extracted by cutting the skin samples into small pieces and stirring them in 10 mL of HS buffer for 18 h. The resultant extract was filtered through 0.45 μm membrane filters and the filtrate quantified for hbFGF by ELISA (see below). The recovery data provided an estimate of the minimum amount of substance retained within the membrane since it was not possible to determine whether complete (i.e., 100%) extraction was achieved.

Transport Studies. *a. Effect of Current Density.* Three different current densities (0.15, 0.3, and 0.5 mA/cm^2) were applied for 8 h using the above-mentioned formulation (0.5 mg/mL hbFGF in HS buffer with 15 mM ACM). $n \geq 4$ in all experiments.

b. Comparing hbFGF Iontophoresis across Porcine and Human Skin. Iontophoretic delivery of hbFGF across porcine and human skin samples was compared under the same experimental conditions: 0.5 mg/mL hbFGF in HS buffer with 15 mM ACM iontophoresed for 8 h at 0.5 mA/cm^2. $n \geq 3$ in all experiments.

c. Determining the Relative Contributions of Electromigration and Electroosmosis to hbFGF Electrotransport and Its Effect on Skin Permselectivity. The contribution of electromigration (EM) to the total flux was calculated as described previously.[4,26] Briefly, the following equations were used:

$$J_{EM} = J_{tot} - J_{EO} \quad (1)$$

where $J_{EO} = V_w C_{hbFGF}$, and

$$V_W = J_{ACM}/C_{ACM} \quad (2)$$

Also,

$$IF = Q_{ACM,control}/Q_{ACM,hbFGF} \quad (3)$$

In the above equations,
J_{tot} = total flux
J_{EM} = flux due to electromigration
J_{EO} = flux due to electroosmotic flow
V_w = linear velocity of solvent flow
C_{hbFGF} = concentration of hbFGF
J_{ACM} = flux of the marker molecule (ACM)
C_{ACM} = donor concentration of the marker molecule (ACM)
IF = inhibition factor
$Q_{ACM,control}$ = cumulative permeation of ACM in 8 h in the absence of hbFGF
$Q_{ACM,hbFGF}$ = cumulative permeation of ACM in 8 h in the presence of hbFGF

Analysis of hbFGF by ELISA. Cumulative permeation and skin deposition of hbFGF were quantified by ELISA (human fibroblast growth factor 2 ELISA kit (CKH123), Cell Sciences; Canton, MA) according to the protocol provided by the supplier. Briefly, after appropriate dilution, 100 μL samples were pipetted into a 96-well ELISA plate that was coated with a capture antibody specific for hbFGF. After incubation for 2.5 h at room temperature, the plate was washed and a biotinylated anti-hbFGF detection antibody (100 μL) added. After incubation at room temperature for 1 h, the plate was washed and HRP-conjugated streptavidin (100 μL) added, followed by incubation for a further 45 min. TMB solution was added after washing the plate, and the reaction was stopped after another 30 min by the addition of 50 μL of 2 M sulfuric acid. The absorbance was read at 450 nm immediately after terminating the reaction. The LOD and LOQ were 5.34 and 16.19 ng/mL, respectively.

Quantifying Biological Activity of hbFGF Using Cell Proliferation Assays. The biological activity of hbFGF postdelivery was determined by quantifying its ability to stimulate the proliferation of (i) human foreskin fibroblast (HFF) cells and (ii) NIH 3T3 cells. The effect of hbFGF that had permeated across the skin or been deposited within the membrane during iontophoresis on cell growth was compared to that of a commercially available hbFGF (F9786, Sigma Aldrich; Buchs, Switzerland) and the protein expressed in-house: these served as positive controls.

a. Human Foreskin Fibroblasts (HFF). The assay was performed using a slightly modified published method.[27] Briefly, cells were grown in D-MEM GlutaMAX media (supplemented with 10% FBS and 1% PenStrep) with cell splitting every 4 days. When the cells had reached 70−80% confluency, they were detached using trypsin and counted using a hemocytometer. The cells (750 in 180 μL) were then dispensed into the wells of a 96-well plate. Sterile 25 mM HEPES 133 mM NaCl (20 μL) was added to the media and cell controls (lanes 1 and 2, respectively). After appropriate dilution, 20 μL aliquots of hbFGF from permeation and skin deposition samples were pipetted into lanes 7 and 8. Lanes 3 to 6 contained the commercially available hbFGF and the hbFGF expressed in-house, which were used as positive controls. The hbFGF concentration was 1.25 μg/mL. Cells were allowed to proliferate for 2, 4, and 6 days before their viability was determined by XTT assay; 50 μL of sterile filtered XTT reagent (1 mg/mL XTT, 17.2 μg/mL menadione, 25 mM HEPES in RPMi media) was added to each well. After incubation for 8 h, the spectrophotometric absorbance of the formazan dye

was read by an ELISA plate reader at a wavelength of 450 nm with a reference point at 750 nm.

b. NIH 3T3 Cell Lines. The assay with NIH 3T3 cells was performed using the same protocol as described above except that cells were grown on D-MEM basal media (again supplemented with 10% FBS and 1% PenStrep).[28] Cells were allowed to proliferate for 2 and 4 days, and the incubation time after adding XTT reagent was 6 h.

HPLC Analysis of Acetaminophen. ACM was analyzed using a P680A LPG-4 pump equipped with an ASI-100 autosampler and a UV/vis detector (UVD 170/340-U) (Dionex; Voisins LeBretonneux, France) and a LiChrospher column packed with 5 μm C18 silica reversed-phase particles. The mobile phase comprised 80% citrate buffer (40 mM; pH 3.0) and 20% methanol. The flow rate was 1 mL/min, column temperature was 30 °C and the injection volume was 25 μL. ACM was detected using its absorbance at 243 nm. The LOD and LOQ were 0.16 and 0.49 μg/mL, respectively.

Preparation of Rhodamine-Tagged hbFGF and Confocal Laser Scanning Microscopy Studies. *a. Experimental Protocol To Label hbFGF.* Purified hbFGF (~10 mg) was dialyzed overnight through a membrane with a molecular weight cutoff of 6−8 kDa into a carbonate−bicarbonate buffer system (100 mM; pH 8.5). The protein concentration was measured after dialysis, and rhodamine isothiocyanate (dissolved in methanol) was added such that the molar ratio of protein:rhodamine remained at 1:25. The tagging reaction was carried out with constant stirring for 2 h in the dark.[29] After completion, the reaction mixture was again dialyzed overnight, this time into HS buffer, through a membrane with a 6−8 kDa cutoff in order to remove unreacted rhodamine isothiocyanate and to change the buffer. Finally, the protein solution was filtered through a centrifugal filtration membrane with a molecular weight cutoff of 5 kDa.

b. Visualizing Rhodamine-Tagged hbFGF in the Skin as a Function of Penetration Depth. Stability of the rhodamine-tagged protein in the presence of skin was first confirmed prior to the permeation experiments; no hydrolysis of the conjugate was observed. Rhodamine-tagged hbFGF was then iontophoresed using the experimental setup described above (see Iontophoretic Setup and Protocol) and using dermatomed porcine skin (250 μm). Control experiments were performed using the same conditions but without applying current. Upon completion of the permeation experiments, the skin samples were removed from the diffusion cells and their epidermal and dermal surfaces cleaned under running water. This was followed by gentle drying and storage overnight at −20 °C. The following day, the skin samples were thawed at room temperature for 45 min and then analyzed in the *XZ*-plane using single photon excitation at 543 nm with 4% laser power (Zeiss 710 2P microscope); the emission filter was fixed at 553−639 nm with a pinhole of 35 μm and a master gain of 650. Images were first recorded at the epidermal and dermal surfaces, the latter detecting the presence of rhodamine-labeled hbFGF at the interface in contact with the receiver phase. In order to visualize penetration of the tagged protein into the skin interior, the samples were then gently tape-stripped starting from the epidermal surface.[30] Three series of 15 strips were removed using book tape (TESA; Hamburg, Germany). Measurements showed that removal of 15, 30, and 45 strips reduced membrane thickness from 250 μm to approximately 200, 150, and 100 μm, respectively. The microscope conditions were kept constant in order to compare the images, which were analyzed by ImageJ software.

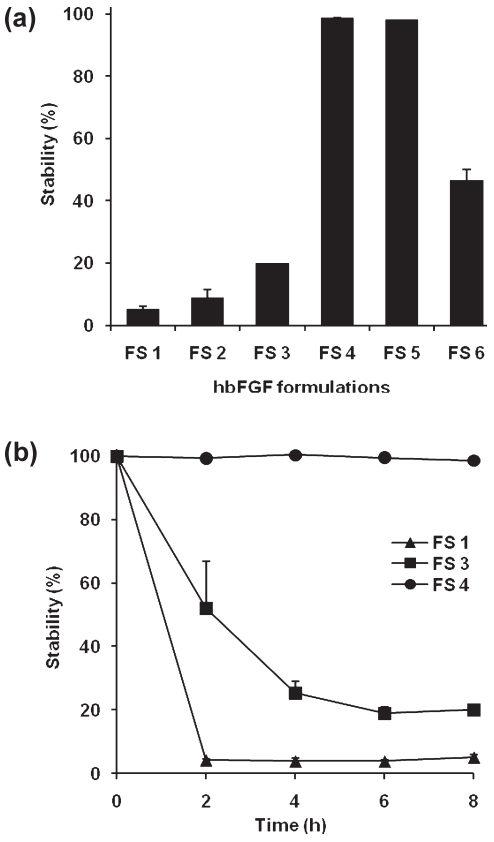

Figure 2. (a) Solution stability of different hbFGF formulations after incubation at room temperature for 8 h (formulation compositions are given in Table 1). (b) Variation of hbFGF in solution as a function of time in formulations FS 1, FS 3 and FS 4 observed during 8 h. Although hbFGF in FS 4 was stable for 8 h, the protein precipitated almost completely within the first 2 h when dissolved in FS 1. Precipitation was slower at higher ionic strength, and hbFGF solubility was ~20% in FS 3 after 6 h and remained so until the end of the study. (Mean ± SD.)

Statistical Analysis. Data were expressed as the mean ± SD. Outliers determined using the Grubbs test were discarded. Results were evaluated statistically using either one-way analysis of variance (ANOVA followed by Student−Newman−Keuls test) or a two-tailed Student *t* test. The level of significance was fixed at $\alpha = 0.05$.

RESULTS

Protein Formulation. Different formulation buffers were prepared (Table 1), and purified hbFGF was directly exchanged into the corresponding formulation buffer using gel filtration chromatography. As a first step, five different formulations were studied with respect to hbFGF stability in solution after 8 h (Figure 2a). Formulations FS 1 and FS 2, which did not contain NaCl, showed the lowest stability (only 5.15 ± 0.88% for FS 1 and 8.73 ± 2.91% for FS 2 of the initial hbFGF concentration was measured in solution after 8 h). For FS 3, which contained 25 mM NaCl buffered at pH 7.4, recovery improved to 19.97 ± 0.17%. Increasing the NaCl concentration to 133 mM at pH 7.4 (FS 4) resulted in maximum stability after incubation for 8 h (98.61 ± 0.08%), which was unchanged when FS 4 was supplemented with 0.01% BSA (FS 5; 98.07 ± 0.16%). Formulation FS 6 was made at an intermediate ionic strength

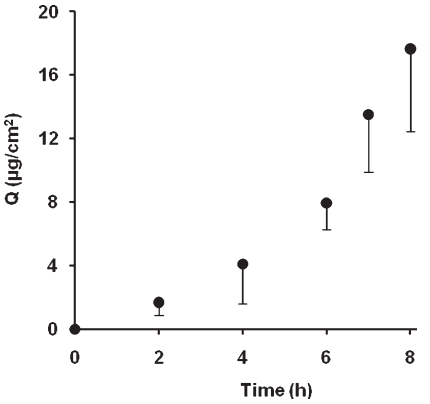

Figure 3. Cumulative hbFGF permeation (Q) as a function of time during 8 h of iontophoresis at 0.5 mA/cm^2. (Mean ± SD, n = 11.)

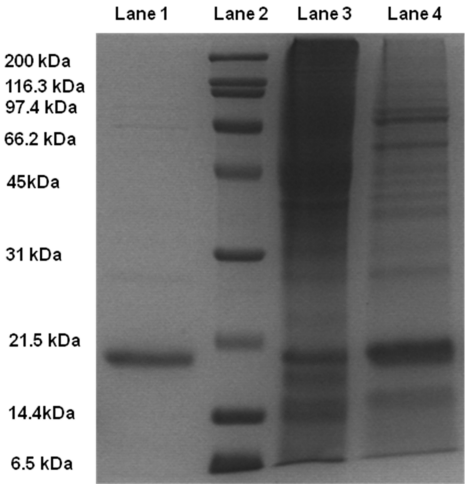

Figure 4. SDS−PAGE (15%) results showing: lane 1, hbFGF standard (control); lane 2, molecular weight markers; lane 3, permeation sample; and lane 4, skin extraction sample. The bands due to hbFGF from samples taken from the receiver compartment and the skin samples postiontophoresis have the same molecular weight as the control giving a qualitative indication that the protein was intact.

(64 mM) and using a different salt (NaH_2PO_4) and had moderate stability (46.5 ± 3.7%).

Formulations FS 1, FS 3, and FS 4 were selected to investigate the variation of hbFGF concentration in solution over 8 h with hbFGF quantification every 2 h (Figure 2b). In the case of FS 1, hbFGF levels decreased rapidly to 4.25 ± 0.26% after only 2 h and remained at this level for the duration of the experiment. Visual inspection revealed that FS 1 was turbid, indicating that the protein had precipitated. Although formulation FS 3 contained 25 mM NaCl, hbFGF levels in solution also decreased rapidly over time, falling to only 20% after 6 h. As indicated by the first series of experiments, FS 4 was stable throughout the study.

Demonstrating the Noninvasive Transdermal Iontophoretic Delivery of hbFGF. Solution stability studies, conducted prior to the iontophoretic transport experiments, confirmed the stability of hbFGF under the experimental conditions to be used. The hbFGF concentration measured in solution after 8 h in the presence of dermis and epidermis and following current application (0.5 mA/cm^2) was 98.1 ± 0.2, 98.6 ± 0.1 and 97.3 ± 0.3%, respectively, of the initial value, indicating that the protein was

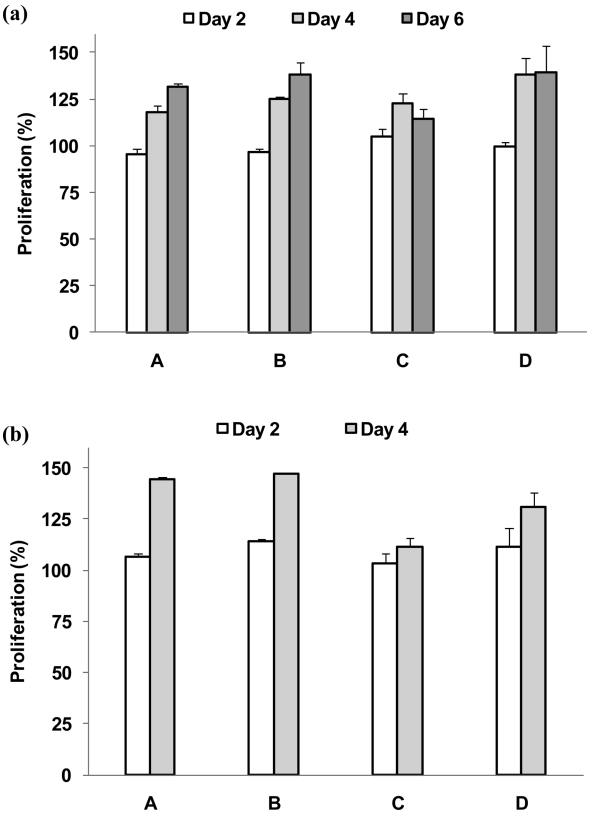

Figure 5. Biological activity of hbFGF was quantified by its ability to stimulate the proliferation of (a) human foreskin fibroblasts (HFF) cells and (b) NIH 3T3 cells. A = commercially available hbFGF (F9786, Sigma Aldrich; Buchs, Switzerland), B = hbFGF expressed in-house, C = hbFGF after permeation across the skin, D = hbFGF deposited within the skin during iontophoresis. Cell growth in the absence of added hbFGF at each time point was taken as the reference (i.e, 100%). (Mean ± SD, $n \geq 5$.)

stable. Cumulative hbFGF permeation and steady state flux following iontophoresis at a current density of 0.5 mA/cm^2 using a formulation containing 0.5 mg/mL hbFGF were 17.64 ± 5.18 μg/cm^2 and 4.85 ± 2.57 μg/cm^2·h, respectively (Figure 3); in addition, 77.74 ± 37.36 μg/cm^2 of hbFGF was deposited in the skin. Thus, permeation and deposition accounted for 18% and 82% of total transport, respectively. SDS−PAGE of permeation and skin extraction samples confirmed that hbFGF remained intact postiontophoresis (Figure 4).[31]

Confirming the Biological Activity of hbFGF Postdelivery. Functional integrity of hbFGF after iontophoretic delivery was demonstrated using HFF and NIH 3T3 cells.[27,28] Figure 5a shows the proliferation of HFF cells after 2, 4, and 6 days in the presence of the commercially available protein (A), hbFGF produced in-house (B) and hbFGF permeated across (C) and deposited within (D) the skin during iontophoresis; cell growth in the absence of additional hbFGF was determined on days 2, 4, and 6 and taken as the reference and considered to be 100% for each time point. No statistical superiority over control was seen on day 2; however, the effect of adding hbFGF on cell proliferation was apparent by day 4 (Figure 5a, light gray bars). The results confirmed that the protein expressed in-house (B) and used in the transport studies possessed comparable activity to the commercially available hbFGF (A). The data also demonstrated that hbFGF from the permeated (C) and extracted (D) samples

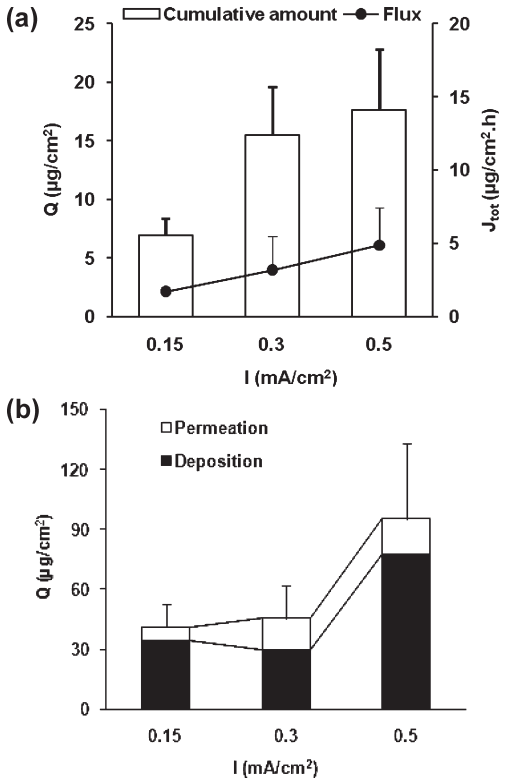

Figure 6. (a) Cumulative permeation (Q) and steady-state flux (J_{tot}) of hbFGF as a function of current density (at 0.15, 0.3, and 0.5 mA/cm^2) across porcine skin after 8 h of transdermal iontophoresis. (Mean ± SD, $n \geq 4$.) (b) Effect of current density on total hbFGF delivery: the sum of the amounts permeated across and retained within the skin. (Mean ± SD, $n \geq 4$.)

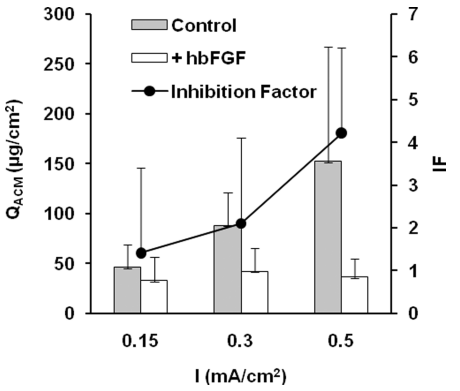

Figure 7. Cumulative acetaminophen (ACM) permeation across the skin after 8 h of transdermal iontophoresis at 0.15, 0.3, and 0.5 mA/cm^2 in the presence and in the absence of hbFGF. The inhibition factors (IF) were calculated using eq 3. (Mean ± SD, $n \geq 4$.)

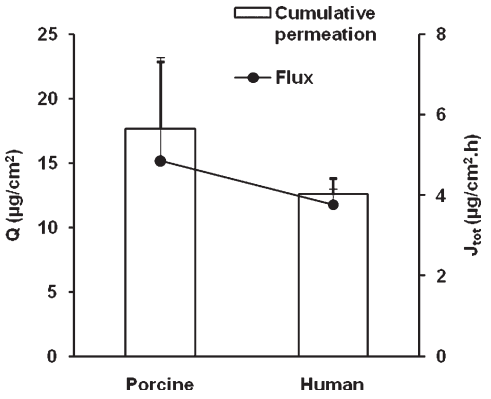

Figure 8. Comparison of cumulative permeation (Q) and steady state flux (J_{tot}) of hbFGF across porcine and human skin after iontophoresis at 0.5 mA/cm^2 for 8 h. (Mean ± SD, $n \geq 3$.)

was biologically active postdelivery and enhanced cell proliferation (growth on day 4 in samples treated with samples C and D was 122.5 ± 5.4% and 138.4 ± 8.7%, respectively, cf. 100% for the controls). The trend was maintained on day 6: cell proliferation for samples C and D was 114.2 ± 5.7% and 139.2 ± 14.2%, respectively, as compared to control (100%) (Figure 5a, dark gray bars); the reason for the slightly decreased rate of proliferation observed on day 6 as compared to day 4 for cells treated with permeation samples (C) remains unclear. The results obtained with the HFF cells were confirmed using NIH 3T3 cells (Figure 5b). Cell proliferation of NIH 3T3 cells on day 4 in the presence of hbFGF from the permeation (C) and extraction (D) samples was 111.2 ± 4.3% and 130.8 ± 7.0%, respectively.

Effect of Current Density on Iontophoretic Delivery Kinetics. Electrotransport was found to be influenced by the applied current density; an increase from 0.15 to 0.3 mA/cm^2 resulted in a proportional increase in cumulative hbFGF permeation (6.93 ± 1.43 and 15.47 ± 4.10 μg/cm^2) and steady state flux (1.71 ± 0.27 and 3.18 ± 2.27 μg/cm^2·h) (Figure 6a). However, a further increase from 0.3 to 0.5 mA/cm^2 did not produce any statistically significant difference in either cumulative permeation or steady state flux ($P < 0.05$; ANOVA followed by Student–Newman–Keuls test) (Figure 6a). Comparison of the amounts permeated and recovered following skin extraction confirmed that appreciable quantities of hbFGF were retained in the skin during iontophoresis at each current density (Figure 6b); the amounts recovered at 0.15, 0.3, and 0.5 mA/cm^2 were 34.14 ± 11.65, 29.97 ± 15.86 and 77.74 ± 37.36 μg/cm^2, respectively. Skin deposition at 0.5 mA/cm^2 was statistically superior to that at the lower current densities ($P < 0.05$; ANOVA followed by Student–Newman–Keuls test).

Effect of hbFGF Electrotransport on Skin Permselectivity. Figure 7 compares the cumulative ACM permeation in the presence and absence of hbFGF; the ratio gives the inhibition factors (IF) at each current density (eq 3), which were 1.41 ± 1.25, 2.10 ± 1.43 and 4.22 ± 3.82 at 0.15, 0.3, and 0.5 mA/cm^2, respectively. The IF values were similar (in the range of 1 to 5) to those calculated previously for cytochrome c and ribonuclease A and indicated that the proteins exerted a modest effect on skin permselectivity and then only at the highest current density.[3,4] For comparison, vapreotide, which binds strongly to the skin, displays an IF of ~50.[26] In addition to directly binding to and hence neutralizing the fixed negative charges in the skin, as the amount of hbFGF in the transport channel increases, it can also screen the fixed negative charges more effectively, thus reducing the double layer thickness and electroosmotic solvent flow, resulting in the increase in the inhibition factor.

Equivalence of Delivery across Porcine and Human Skin. Comparison of hbFGF delivery across human and porcine skin under the same iontophoretic conditions (8 h current application at 0.5 mA/cm^2) showed that cumulative permeation (12.57 ± 1.26 and 17.64 ± 5.18 μg/cm^2) as well as steady state flux

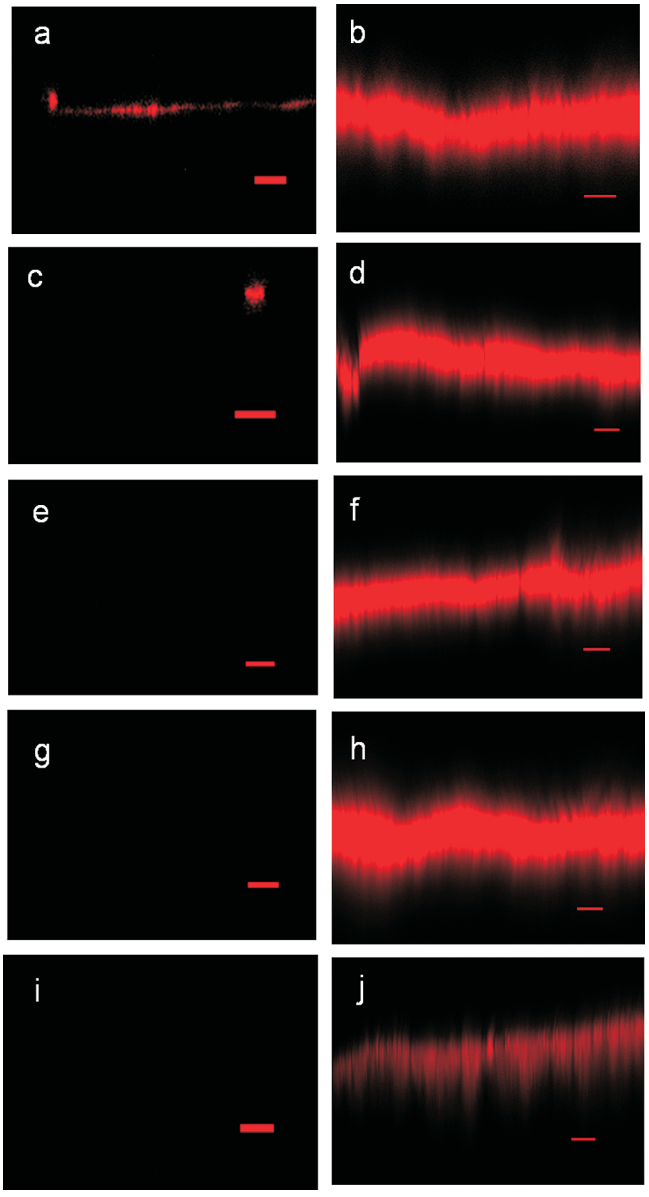

Figure 9. Confocal laser scanning microscopy images of rhodamine-tagged hbFGF from porcine skin following either passive diffusion for 8 h (a, c, e, g and i) or 8 h of constant current iontophoresis at 0.5 mA/cm^2 (b, d, f, h and j). The images are taken at the skin surface (a, b) and after removing 15 (c, d), 30 (e, f) and 45 (g, h) tape-strips, respectively. The final pair of images (i and j) was recorded after inverting the skin samples and show the fluorescence intensity at the dermal surface (which was in contact with the receiver solution). (Red scale bar = 50 μm.)

(3.76 ± 0.40 and 4.85 ± 2.57 μg/cm^2·h) across human and porcine skin, respectively, were statistically equivalent (t (1.64) < t_{crit} (2.18); Student t test) (Figure 8).

Confocal Laser Scanning Microscopy Images of Protein Distribution in Skin. Figure 9 shows single photon CLSM images in the *XZ*-plane comparing passive (panels a, c, e, g, i) and iontophoretic delivery (panels b, d, f, h, j) of rhodamine-tagged hbFGF as a function of depth. Figure 9a (epidermal surface: no tape-strips) shows fluorescence due to rhodamine-labeled hbFGF at the skin surface; no labeled hbFGF was observed in the skin samples after removal of 15 (Figure 9c), 30 (Figure 9e) or 45 (Figure 9g) tape-strips or at the dermal surface (Figure 9i). In contrast, the images following iontophoresis (Figure 9: panel b, skin surface; panel d, 15 tape-strips (~50 μm); panel f, 30 tape-strips (~100 μm); panel h, 45 tape-strips (~150 μm); panel j, dermal surface) give striking visual evidence that iontophoretic current application enabled deep permeation of the rhodamine-tagged hbFGF. Covalently tagged rhodamine conjugate was stable in the presence of skin as no fluorescence was observed in the dialyzed sample. Semiquantitative data analysis showed that postiontophoretic fluorescence intensity of tagged hbFGF at the skin surface (243.4 ± 25.0 AU) was superior to that in the absence of current (59.9 ± 43.6 AU). After removal of 30 tape-strips, in contrast to the control, strong fluorescence was still clearly seen in the dermis after iontophoresis (241.6 ± 25.7 AU). Thus, following iontophoresis, the fluorescence intensity remained effectively constant as a function of depth except in the last image (Figure 9j), which might be due to a sink effect with tagged protein migrating to the receptor solution.

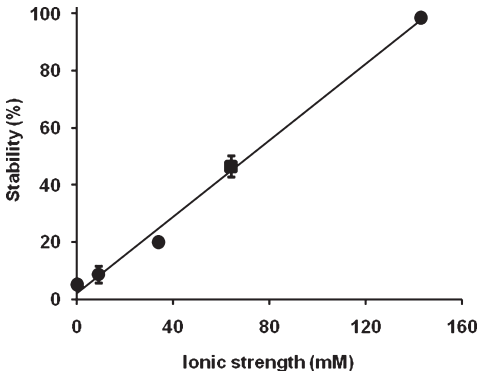

Figure 10. Solution stability (%) of hbFGF plotted against ionic strength of the formulation indicates a strong correlation (R^2 > 0.99). Formulation FS 6 (filled square) at an intermediate ionic strength of 64 mM containing NaH_2PO_4 had a predicted stability of ~45% which corresponded well to the experimentally determined value of 46.5 ± 3.7%.

DISCUSSION

Effect of Ionic Strength on hbFGF Formulation Stability. Development of a viable hbFGF delivery system will require a formulation that ensures that the protein does not precipitate and that it retains its structure and function. Moreover, from a toxicological point of view, precipitated or aggregated protein can lead to immunological reactions.[32,33] Increasing NaCl concentration from 25 mM (FS 3) to 133 mM at pH 7.4 (FS 4) resulted in improved stability of hbFGF in solution after incubation for 8 h, which was unchanged when FS 4 was supplemented with 0.01% BSA (FS 5). These observations indicated that ionic strength was an important factor in maintaining hbFGF in solution. Indeed, a plot of percentage hbFGF stability against ionic strength for the formulations yielded a strong correlation (R^2 > 0.99) (Figure 10). The validity of the hypothesis was challenged by comparing the predicted and experimentally determined solution stabilities at 8 h of a hbFGF formulation (FS 6) at an intermediate ionic strength (64 mM) and using a different salt (NaH_2PO_4). The predicted stability (~45%) calculated using the regression equation derived from the data in Figure 10 showed excellent agreement with the experimentally determined value of 46.5 ± 3.7%. Thus, it seems that the stability of hbFGF in solution depends strongly on the ionic strength of the formulation

Table 2. Iontophoretic Transport Parameters for hbFGF and the Relative Contributions of Electromigration (EM) and Electroosmosis (EO) ($n \geq 4$)

				$10^3 V_w$[c]		
I[a] (mA/cm^2)	J_{tot}[b] (μg/cm^2·h)	EM (%)	EO (%)	hbFGF (cm/h)	control (cm/h)	IF[d]
0.15	1.71 ± 0.27	38	62	2.13 ± 1.20	2.80 ± 1.59	1.41 ± 1.25
0.3	3.18 ± 2.27	61	39	2.45 ± 1.63	6.48 ± 2.20	2.10 ± 1.43
0.5	4.85 ± 2.57	75	25	2.45 ± 1.10	6.15 ± 3.10	4.22 ± 3.82

[a] I: Current density. [b] J_{tot}: Total steady-state flux. [c] V_w: Linear velocity of solvent flow. [d] IF: Inhibition factor (calculated according to eq 3).

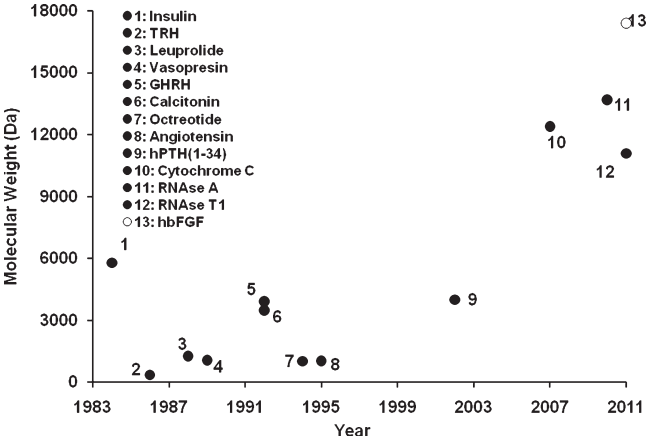

Figure 11. A chronology of the studies into the transdermal iontophoretic delivery of different peptides and proteins showing the evolution in the size of the molecules under investigation. (Nonexhaustive compilation.)[3,4,36−45] To date, hbFGF (17.4 kDa; open circle) is the largest (functional) protein delivered by iontophoresis across intact skin.

but not necessarily on the type of salt (at least with respect to NaCl and NaH_2PO_4), and that the protein shows greater stability at physiological ionic strength. Iontophoretic delivery efficiency is optimal in the so-called "single-ion case", that is, in the absence of competing charge carriers, such as NaCl.[34] However, as seen for hbFGF, the solution stability of biomolecules frequently depends on the presence of salts, including NaCl, or other stabilizers and solutions having an optimal ionic strength. Since formulation stability is the priority, iontophoretic delivery parameters need to be adapted to reach a satisfactory compromise.

Iontophoretic Transport of Biologically Active hbFGF. The iontophoretic transport data and subsequent cell proliferation studies with the HFF and NIH 3T3 cells demonstrated that intact, biologically active hbFGF was delivered noninvasively into and across the skin. Not only is structural and functional integrity obviously essential to elicit pharmacological effect, it also reduces the risk of unwanted immunological reactions.

As mentioned above, hbFGF skin deposition was significantly greater than permeation at each current density, accounting for 83.1, 65.9 and 81.5% of total hbFGF delivery at 0.15, 0.3, and 0.5 mA/cm^2, respectively. Thus, it may be possible to target hbFGF delivery preferentially to the epidermis and dermis, which would be an advantage for the treatment of dermatological conditions. Although there was a proportional increase in hbFGF cumulative permeation on increasing current density from 0.15 to 0.3 mA/cm^2, there was no statistically significant improvement at 0.5 mA/cm^2 (Figure 6a). As current density is increased and more hbFGF is driven into the skin, the transport pathways may become saturated with protein and concentration polarization may prevent further increases in permeation in response to increases in the applied current density. However, there was an increase in skin deposition—the amount of hbFGF recovered at 0.5 mA/cm^2 was ~2.6-fold higher than that at 0.3 mA/cm^2 (77.74 ± 37.36 and 29.97 ± 15.86 μg/cm^2, respectively)—this provides further support for the hypothesis that protein can enter the skin but its diffusion in the transport pathway is limited. It should be noted that the maximum current density used in these experiments, 0.5 mA/cm^2, is considered as acceptable for human use with the proviso that the application area is not too large.[35] Statistically equivalent delivery across porcine and freshly excised human skin not only validated the use of the former as a good model for human skin[20−23] but also confirmed that constant current iontophoresis was able to deliver hbFGF across intact human skin.

Electrotransport Mechanism Governed by Current Density. Despite their molecular weight, the principal electrotransport mechanism for both cytochrome *c* and ribonuclease A was found to be electromigration.[3,4] The situation for hbFGF seems more complex since the dominant mechanism was dependent upon current density (Table 2). Using eqs 1 and 2, the contribution of electromigration was calculated and it was the major driving force at 0.3 and 0.5 mA/cm^2, accounting for 61 and 75% of the total flux. However, electroosmosis was the dominant mechanism (responsible for 62% of total transport) at the lowest current density tested (0.15 mA/cm^2).

Significance of hbFGF Delivery: Is There a Molecular Size Limit for Iontophoretic Protein Transport? The earliest investigations into the iontophoretic delivery of insulin (MW ~5.8 kDa) were made approximately a quarter of a century ago.[36] They stimulated research into the delivery of other "biopharmaceuticals", mostly smaller peptide hormones (and their analogues) (Figure 11).[1,2,37−44] It was generally considered that the iontophoretic delivery of larger peptides or proteins across intact skin was not feasible since electrotransport of higher molecular weight species was dependent on electroosmosis and convective solvent flow driven transport was insufficient to overcome the diffusional resistance of the stratum corneum.[1] However, in recent years, we have reported the successful iontophoretic delivery of cytochrome *c* (12.4 kDa), RNase A (13.6 kDa) and RNase T1 (11.1 kDa); the latter two were also shown to have retained their biological activity postdelivery.[3,4,45] The successful delivery of 17.4 kDa hbFGF now encourages us to investigate the transport of larger proteins that were previously considered to be beyond the scope of this delivery technology.

Is Therapeutic Delivery of hbFGF Possible Using Iontophoresis? Under the experimental conditions used in this study, total hbFGF delivery ranged from 41 ± 11 to 95 ± 37 μg/cm^2 at 0.15 and 0.5 mA/cm^2, respectively. Based on earlier clinical trials,

these amounts appear to be in the clinically useful window for the treatment of a number of conditions. For example, topical application of an hbFGF spray (30 μg over 6−30 cm^2) for the treatment of burns in adult and pediatric patients found an improvement in scar quality and faster healing rates.[10−12] Although dose titration studies are scarce, experiments in Yorkshire swine using hbFGF for the stimulation of epidermal wound healing found that bFGF was equally effective at doses of 1 and 10 μg but not at 0.1 μg.[46] Thus, it would appear that microgram amounts of hbFGF are sufficient for pharmacological effect. Furthermore, intradermal injection of hbFGF at 0.1 and 1.0 μg/cm suture in patients with acute incisional scars produced a good or excellent clinical response in 70% (21 out of 30) and 82% (82 out of 100) of patients, respectively.[14] In a recent phase 1 clinical trial, arterial infusion of 100 μg of hbFGF absorbed into 3 mg of acidic gelatin hydrogel microspheres was used to treat peripheral arterial disease; all patients (n = 8) showed an improvement (albeit sometimes temporary) in symptoms.[16] Although electrically assisted delivery may not be essential to administer hbFGF in wounds or other conditions where the stratum corneum is absent and barrier function compromised, it does offer a patient-friendly alternative to intradermal injection or intra-arterial infusion. Recent fundamental studies have also suggested that hbFGF is a potent inhibitor of terminal mesodermal differentiation and the formation of myofibroblasts and thus may have a role in the treatment of keloids; current therapeutic approaches involve direct injection into these areas of hyperproliferative growth which can be painful.[47,48] The specific iontophoretic conditions, including the current density, duration and profile of current application and the application area, which influence hbFGF delivery must be optimized, but the results presented here point to the feasibility of administering therapeutic amounts of hbFGF. Although clinical studies involving continuous or pulsatile iontophoresis of both low molecular weight therapeutics and peptides for 24 h have been reported and shown that iontophoretic patches were well-tolerated, local administration of the protein would require shorter, perhaps intermittent, application periods; this has been suggested as a means to reduce the risk of local irritation.[2,49−51]

CONCLUSION

The results demonstrate the feasibility of using transdermal iontophoresis to deliver correctly folded, biologically active human basic fibroblast growth factor, a 17.4 kDa protein, into and across the skin. They underline the potential of the technology to enable noninvasive protein delivery via the patient-friendly transdermal route. The electrotransport mechanism was found to be current-dependent—electromigration at current densities $\geq$0.3 mA/cm^2—whereas at 0.15 mA/cm^2, transport was principally due to electroosmosis. Use of the higher current densities also appeared to favor skin deposition over permeation, perhaps an advantage for dermatological applications. The amounts of hbFGF delivered by iontophoresis were in the therapeutic range and corresponded to those used in clinical trials and animal studies for the treatment of burns, incisional wounds, recalcitrant ulcers and peripheral arterial disease. As a next step, the iontophoretic delivery of hbFGF will be evaluated *in vivo* in an animal model. Future mechanistic studies will focus on elucidating the role of protein structure and the three-dimensional distribution of physicochemical properties on protein electrotransport.

ASSOCIATED CONTENT

Supporting Information. Additional experimental details, table of purification steps for the production of hbFGF, and figures depicting purification of hbFGF and characterization of partially purified protein by mass analysis. This material is available free of charge via the Internet at http://pubs.acs.org.

AUTHOR INFORMATION

Corresponding Author

*School of Pharmaceutical Sciences, University of Geneva, 30 Quai Ernest Ansermet, 1211 Geneva 4, Switzerland. Tel: +41 22 379 3355. Fax: +41 22 379 3360. E-mail: yogi.kalia@unige.ch.

ACKNOWLEDGMENT

We would like to thank Dr. Anis Feki (Department of Obstetrics and Gynecology, University Hospital, Geneva) for providing pWPI_SPbFGF harboring the *bfgf* gene. We also thank Nathalie Oudry and Prof. Gerard Hopfgartner from the High Resolution Mass Spectrometry Platform of the Faculty of Science, University of Geneva, for the MALDI-TOF spectra. We would also like to acknowledge Dr. Christoph Bauer and Jerome Bosset of the Bioimaging Platform of the NCCR "Frontiers in Genetics" at the University of Geneva for their help with confocal microscopy and Kim Schneider, Surekha Pimple and Pernilla Hoffmann for providing the cell lines for the study and for their assistance with the cell culture experiments. Finally, we would like to thank Dr. Kouroche Amini, Department of Plastic, Aesthetic and Reconstructive Surgery, Geneva University Hospital, for providing human skin samples.

REFERENCES

(1) Kalia, Y. N.; Naik, A.; Garrison, J.; Guy, R. H. Iontophoretic drug delivery. *Adv. Drug Delivery Rev.* **2004**, *56*, 619–658.

(2) Green, P. G. Iontophoretic delivery of peptide drugs. *J. Controlled Release* **1996**, *41*, 33–48.

(3) Cazares-Delgadillo, J.; Naik, A.; Ganem-Rondero., A.; Quintanar-Guerrero., D.; Kalia, Y. N. Transdermal delivery of cytochrome C—a 12.4 kDa protein—across Intact skin by constant-current iontophoresis. *Pharm. Res.* **2007**, *24*, 1360–1368.

(4) Dubey, S.; Kalia, Y. N. Non-invasive iontophoretic delivery of enzymatically active ribonuclease A (13.6 kDa) across intact porcine and human skins. *J. Controlled Release* **2010**, *145*, 203–209.

(5) Zhang, J.; Cousenst, L. S.; Barrt, P. J.; Sprang, S. R. Three-dimensional structure of human basic fibroblast growth factor, a structural homolog of interleukin 1β. *Proc. Natl. Acad. Sci. U.S.A.* **1991**, *88*, 3446–3450.

(6) Kurokawa, I.; Hayami, J.; Kita, Y. A therapy-resistant chronic leg ulcer treated successfully with topical basic fibroblast growth factor. *J. Int. Med. Res.* **2003**, *31*, 149–151.

(7) Yamanaka, K.; Inaba, T.; Nomura, E.; Hurwitz, D.; Jones, D. A.; Hakamada, A.; Isoda, K.; Kupper, T. S.; Mizutani, H. Basic fibroblast growth factor treatment for skin ulcerations in scleroderma. *Cutis* **2005**, *76*, 373–376.

(8) O'Goshi, K.; Tagami, H. Basic fibroblast growth factor treatment for various types of recalcitrant skin ulcers: Reports of nine cases. *J. Dermatol. Treat.* **2007**, *18*, 375–381.

(9) Uchi, H.; Igarashi, A.; Urabe, K.; Koga, T.; Nakayama, J.; Kawamori, R.; Tamaki, K.; Hirakata, H.; Ohura, T.; Furue, M. Clinical efficacy of basic fibroblast growth factor (bFGF) for diabetic ulcer. *Eur. J. Dermatol.* **2009**, *19*, 461–468.

(10) Akita, S.; Akino, K.; Imaizumi, T.; Hirano, A. A fibroblast growth factor improved the quality of skin grafting in burn patients. *Burns* **2005**, *31*, 855–858.
(11) Akita, S.; Akino, K.; Imaizumi, T.; Tanaka, K.; Anraku, K.; Yano, H.; Hirano, A. The quality of pediatric burn scars is improved by early administration of basic fibroblast growth factor. *J. Burn Care Res.* **2006**, *27*, 333–338.
(12) Akita, S.; Akino, K.; Imaizumi, T.; Hirano, A. Basic fibroblast growth factor accelerates and improves second-degree burn wound healing. *Wound Repair Regen.* **2008**, *16*, 635–641.
(13) Akasaka, Y; Ono, I.; Yamashita, T; Jimbow, K; Ishii, T. Basic fibroblast growth factor promotes apoptosis and suppresses granulation tissue formation in acute incisional wounds. *J. Pathol.* **2004**, *203*, 710–720.
(14) Ono, I.; Akasaka, Y.; Kikuchi, R.; Sakemoto, A.; Kamiya, T.; Yamashita, T.; Jimbow, K. Basic fibroblast growth factor reduces scar formation in acute incisional wounds. *Wound Repair Regen.* **2007**, *16*, 617–623.
(15) Lazarous, D. F.; Unger, E. F.; Epstein, S. E.; Stine, A.; Arevalo, J. L.; Chew, E. Y.; Quyyumi, A. Basic fibroblast growth factor in patients with intermittent claudication: results of a phase I trial. *J. Am. Coll. Cardiol.* **2000**, *36*, 1239–1244.
(16) Hashimoto, T.; Koyama, H.; Miyata, T.; Hosaka, A.; Tabata, Y.; Takato, T.; Nagawa, H. Selective and sustained delivery of basic fibroblast growth factor (bFGF) for treatment of peripheral arterial disease: Results of a phase I trial. *Eur. J. Vasc. Endovasc. Surg.* **2009**, *38*, 71–75.
(17) Mazué, G.; Bertolero, F.; Jacob, C.; Sarmientos, P.; Ronucci, R. Preclinical and clinical studies with recombinant human basic fibroblast growth factor. *Ann. N.Y. Acad. Sci.* **1991**, *638*, 329–340.
(18) Casey, R.; Li, W. W. Factors controlling ocular angiogenesis. *Am. J. Ophthalmol.* **1997**, *124*, 521–529.
(19) Sharp, P. S. The role of growth factors in the development of diabetic retinopathy. *Metabolism* **1995**, *44*, 72–75.
(20) Dick, I. P.; Scott, R. C. Pig ear skin as an *in vitro* model for human skin permeability. *J. Pharm. Pharmacol.* **1992**, *44*, 640–645.
(21) Simon, G. A.; Maibach, H. I. The pig as an experimental model of percutaneous permeation in man: Qualitative and quantitative observations — an overview. *Skin Pharmacol. Appl. Skin Physiol.* **2000**, *13*, 229–234.
(22) Sekkat, N.; Kalia, Y. N.; Guy, R. H. Biophysical study of porcine ear skin *in vitro* and its comparison to human skin *in vivo*. *J. Pharm. Sci.* **2002**, *91*, 2376–2381.
(23) Jacobi, U.; Kaiser, M.; Toll, R.; Mangelsdorf, S.; Audring, H.; Otberg, N.; Sterry, W.; Lademann, J. Porcine ear skin: an *in vitro* model for human skin. *Skin Res. Technol.* **2007**, *13*, 19–24.
(24) Franz, T. J. Percutaneous absorption. On the relevance of *in vitro* data. *J. Invest. Dermatol.* **1975**, *64*, 190–195.
(25) Harrison, S. M.; Barry, B. W.; Dugard, P. H. Effect of freezing on human skin permeability. *J. Pharm. Pharmacol.* **1984**, *36*, 261–262.
(26) Schuetz, Y. B.; Naik, A.; Guy, R. H.; Vuaridel, E.; Kalia, Y. N. Transdermal iontophoretic delivery of vapreotide acetate across porcine skin *in vitro*. *Pharm. Res.* **2005**, *22*, 1305–1312.
(27) Ho, Y. C.; Mi, F. L.; Sung, H. W.; Kuo, P. L. Heparin-functionalized chitosan—alginate scaffolds for controlled release of growth factor. *Int. J. Pharm.* **2009**, *376*, 69–75.
(28) Shen, H.; Hu, X.; Yang, F.; Bei, J.; Wang, S. Cell affinity for bFGF immobilized heparin-containing poly(lactide-co-glycolide) scaffolds. *Biomaterials* **2011**, *32*, 3404–3412.
(29) Smith, M. L.; Carski, T. R.; Griffin, C. W. Modification of fluorescent-antibody procedures employing crystalline tetramethylrhodamine isothiocyanate. *J. Bacteriol.* **1962**, *83*, 1358–1359.
(30) Kalia, Y. N.; Pirot, F.; Guy, R. H. Homogeneous transport in a heterogeneous membrane: water diffusion across human stratum corneum *in vivo*. *Biophys. J.* **1996**, *71*, 2692–2700.
(31) Laemmli, U. K. Cleavage of structural proteins during assembly of the head of bacteriophage T4. *Nature* **1970**, *277*, 680–685.
(32) Rosenberg, A. S. Effects of protein aggregates: an immunologic perspective. *AAPS J.* **2006**, *8*, E501–E507.
(33) Schellekens, H. Factors influencing the immunogenicity of therapeutic proteins. *Nephrol., Dial., Transplant.* **2005**, *20*, 3–9.
(34) Kasting, G. B.; Keister, J. C. Application of electrodiffusion theory for a homogeneous membrane to iontophoretic transport through skin. *J. Controlled Release* **1989**, *8*, 195–210.
(35) Ledger, P. W. Skin biological issues in electrically enhanced transdermal delivery. *Adv. Drug Delivery Rev.* **1992**, *9*, 287–307.
(36) Stephen, R. L.; Petelenz, T. J.; Jacobsen, S. C. Potential novel methods for insulin administration: I. Iontophoresis. *Biomed. Biochem. Acta* **1984**, *43*, 553–558.
(37) Burnette, R. R.; Shen, D. M. Comparison between the iontophoretic and passive transport of thyrotropin releasing hormone across excised nude mouse skin. *J. Pharm. Sci.* **1986**, *75*, 738–743.
(38) Meyer, B. R.; Kreis, W.; Eschbach, J.; O'Mara, V.; Rosen., S.; Sibalis, D. Successful transdermal administration of therapeutic doses of a polypeptide to normal human volunteers. *Clin. Pharmacol. Ther.* **1988**, *44*, 607–612.
(39) Banerjee, P. S.; Ritschel, W. A. Transdermal permeation of vasopressin. I. Influence of pH, concentration, shaving and surfactant on *in vitro* permeation. *Int. J. Pharm.* **1989**, *49*, 189–197.
(40) Kumar, S.; Char, H.; Patel, S.; Piemontese, D.; Iqbal, K.; Malick, A. W.; Neugroschel, E.; Behl, C. R. Effect of iontophoresis on *in vitro* skin permeation of an analogue of growth hormone releasing factor in the hairless guinea pig model. *J. Pharm. Sci.* **1992**, *81*, 635–639.
(41) Morimoto, K.; Iwakura, Y.; Nakatani, E.; Miyazaki, M.; Tojima, H. Effects of proteolytic enzyme inhibitors as absorption enhancers on the transdermal iontophoretic delivery of calcitonin in rats. *J. Pharm. Pharmacol.* **1992**, *44*, 216–218.
(42) Lau, D. T.; Sharkey, J. W.; Petryk, L.; Mancuso, F. A.; Yu, Z.; Tse, F. L. S. Effect of current magnitude and drug concentration on iontophoretic delivery of octreotide acetate (Sandostatin®) in the rabbit. *Pharm. Res.* **1994**, *11*, 1742–1746.
(43) Clemessy, M.; Couarraze, G.; Bevan, B.; Puisieux, F. Mechanisms involved in iontophoretic transport of angiotensin. *Pharm. Res.* **1995**, *12*, 998–1002.
(44) Suzuki, Y.; Nagase, Y.; Iga, K.; Kawase, M.; Oka, M.; Yanai, S.; Matsumoto, Y.; Nakagawa, S.; Fukuda, T.; Adachi, H.; Higo, N.; Ogawa, Y. Prevention of bone loss in ovariectomized rats by pulsatile transdermal iontophoretic administration of human PTH(1—34). *J. Pharm. Sci.* **2002**, *91*, 350–361.
(45) Dubey, S.; Kalia, Y. N. Electrically-assisted delivery of an anionic protein across intact skin: iontophoresis of biologically active Ribonuclease T1. *J. Controlled Release* **2011**, *152* (3), 356–362.
(46) Hebda, P. A.; Klingbeil, C. K.; Abraham, J. A.; Fiddes, J. C. Basic fibroblast growth factor stimulation of epidermal wound healing in pigs. *J. Invest. Dermatol.* **1990**, *95*, 626–631.
(47) Tiede, S.; Ernst, N.; Bayat, A.; Paus, R.; Tronnier, V.; Zechel, C. Basic fibroblast growth factor: A potential new therapeutic tool for the treatment of hypertrophic and keloid scars. *Ann. Anat.* **2009**, *191*, 33–44.
(48) Kelly, A. P. Medical and surgical therapies for keloids. *Dermatol. Ther.* **2004**, *17*, 212–218.
(49) Gupta, S. K.; Southam, M.; Sathyan, G.; Klausener, M. Effect of current density on pharmacokinetics following continuous or intermittent input from a fentanyl electrotransport system. *J. Pharm. Sci.* **1998**, *87*, 976–981.
(50) Viscusi, E. R.; Reynolds, L.; Chung, F.; Atkinson, L. E.; Khanna, S. Patient controlled transdermal fentanyl hydrochloride vs. intravenous morphine pump for postoperative pain. *JAMA, J. Am. Med. Assoc.* **2004**, *291*, 1333–1341.
(51) Kanebako, M.; Inagi, T.; Takayama, K. Evaluation of skin barrier function using direct current II: effects of duty cycle, waveform, frequency and mode. *Biol. Pharm. Bull.* **2002**, *25*, 1623–1628.